

TOPOGRAPHIC RESPONSE TO EXTENSION OF AN OBLIQUE TRAINING JETTY AT IMAGIRE-GUCHI TIDAL INLET

Takaaki Uda¹, Yutaka Ohashi², Toshiro San-nami³, Seiji Kainuma⁴ and Toshinori Ishikawa³

At Imagire-guchi tidal inlet connecting Lake Hamana to the Pacific Ocean, a jetty had been extended by 1973 to stabilize the entrance channel of the inlet. Although 45 years has passed from the completion of the extension of the jetty to 2018, large topographic changes are still occurring offshore of the tidal inlet. One of the authors investigated the topographic changes until 2005, and the beach changes around the inlet were analyzed using the BG model (a model for predicting 3-D beach changes based on Bagnold's concept). In this study, topographic changes were analyzed again using the bathymetric survey data collected by 2017, and the development and deformation of the ebb tidal delta were studied.

Keywords: tidal inlet; topographic changes; Imagire-guchi; Lake Hamana; bathymetric survey data

INTRODUCTION

Lake Hamana with an area of 64.91 km² and a mean water depth of 4.8 m is connected to the Pacific Ocean at Imagire-guchi tidal inlet, as shown in Fig. 1. Since this inlet is located on the western marginal coastline of the Tenryu River delta, westward longshore sand transport prevails near the inlet. Simultaneously, a strong offshore current is generated by the ebb tidal current from the lake, resulting in sand movement in the direction normal to the coastline. Thus, sand transport owing to the westward longshore current is superimposed on the sand movement due to the ebb tidal current offshore of this inlet. At this inlet, an oblique training jetty had been constructed by 1973 to stabilize the inlet. Although 45 years has passed from the completion of the training jetty to 2018, significant topographic changes still continue to occur offshore of the tidal inlet. Tung et al. (2007) predicted the evolution of ebb tidal deltas using the Delft 3-D model. In their model, the full equations of waves and nearshore and tidal currents were solved to predict 3-D bathymetric changes. For practical applications, however, the development of a model by which bathymetric changes can be easily predicted and used to investigate measures against beach erosion is also desirable. Uda et al. (2018) investigated topographic changes around this inlet using eight sets of bathymetric survey data collected between 1964 and 2005, and clarified the development of the ebb tidal delta and developed a model for predicting topographic changes of an ebb tidal delta using the BG model (a model for predicting 3-D beach changes based on Bagnold's concept). According to these studies, topographic changes until 2005 were explained well by the BG model. Since then, topographic changes owing to the ebb tidal current have still continued. In this study, topographic changes including the data set collected until 2017 were investigated, and the development and deformation of the ebb tidal delta were studied again using these field data. Regarding wave characteristics around the inlet, the energy mean significant wave height was 1.32 m and the wave period was 6.4 s according to the wave data collected between 1998 and 2018 at Ryuyo observatory installed at 40 m depth and located 2 km offshore of the coast, and the energy mean wave direction was N187°E. The tide level has been measured at Maisaka Port inside the inlet, and the mean sea level of the spring tide was +0.614 m.

BATHYMETRY AROUND IMAGIRE-GUCHI TIDAL INLET

In the study area, a bathymetric survey has been carried out once a year at 100 m intervals alongshore. In this study, bathymetric survey data collected eleven times between 1964 and 2017 were analyzed, selecting the rectangular area, as shown in Fig. 1, as the study area. First, a channel connecting the lake with the Pacific Ocean and a parallel jetty had already been constructed by 1964 (Fig. 2a). At that time, a deep channel of the inlet was located near the left bank, and a straight channel extended offshore of the inlet. In the offshore zone, the 3–4 m depth contours protruded asymmetrically in the east-west direction while forming a large-scale terrace topography offshore of the inlet, and the tip of the foreset slope of the offshore flat terrace was located at approximately 5 m depth. Since this depth was smaller than the depth of closure (approximately 10 m) of this coast, westward longshore

¹ Public Works Research Center, 1-6-4 Taito, Taito, Tokyo 110-0016, Japan

² Fukuroi Public Works Office, Shizuoka Prefectural Government, 2-1 Yamana, Fukuroi, Shizuoka 437-0042, Japan

³ Coastal Engineering Laboratory Co., Ltd., 1-22-301 Wakaba, Shinjuku, Tokyo 160-0011, Japan

⁴ River Management Division, Transportation Infrastructure Department, Shizuoka Prefectural Government, 9-6 Otemachi, Aoi, Shizuoka 420-8601, Japan

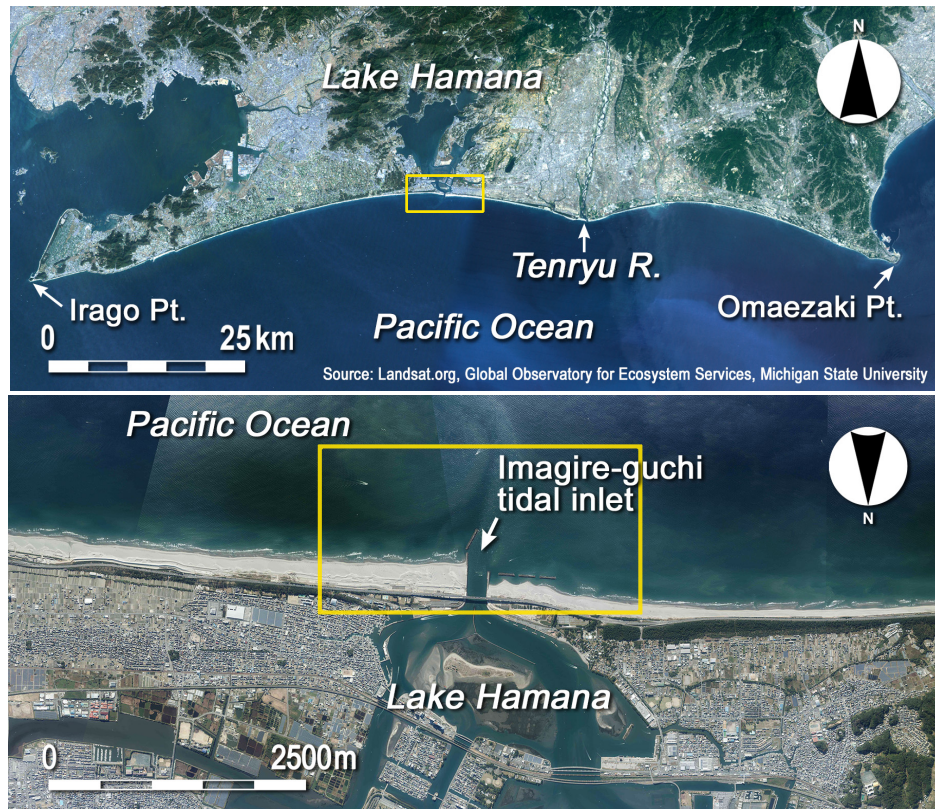


Figure 1. Location of Imagire-guchi tidal inlet facing the Pacific Ocean.

sand transport was able to reach downcoast through the flat terrace and the foreset slope in principle. However, in fact, the westward longshore sand transport was partially blocked by the inlet, and the shoreline and offshore contours between 5 and 10 m depths retreated west of the inlet.

By 1973, a training jetty of 200 m length had been extended obliquely on the left bank in the direction normal to the shoreline with a narrow gap at the tip of the training jetty, which had been constructed by 1968, as shown in Fig. 2b. Owing to the extension of the oblique jetty, the ebb tidal current flowed out obliquely from the inlet, and most furtherly protruding point of the contours shifted west by 200 m relative to the centerline of the offshore terrace, the water depth at the tip of the foreset slope reached 10 m, and the ebb tidal delta significantly protruded offshore. Because the westward longshore sand transport was further blocked by the protrusion, the shoreline significantly receded west of the inlet.

By 1978, a deep channel along the oblique jetty had extended offshore, as shown in Fig. 2c, and an elliptic shoal was formed west of the channel at the same time. The foreset slope of the ebb tidal delta further developed, and the water depth at the tip of the foreset slope reached 12 m. Because this depth was approximately equal to the depth of closure on this coast, the blocking rate of longshore sand transport increased, resulting in downcoast shoreline recession. The shape of the contour line of 10 m depth was asymmetric with respect to the centerline of the delta in the east-west direction, and the contour line markedly retreated on the west side. Also, large scouring holes with a maximum depth of 10 m were formed at the tips of the jetties on both sides.

In 1985, a shoal that extended approximately normal to the shoreline until 1978 deformed, and a deep, large-scale trough was formed west of the inlet, as shown in Fig. 2d, and the ebb tidal delta shifted westward as a whole. In addition, sand was transported offshore and deposited up to a depth of 13 m. By 1990, two detached breakwaters had been constructed immediately west of the inlet with another one under construction, as shown in Fig. 2e. Behind these breakwaters, the shoreline advanced, whereas the shoreline retreated immediately west of the breakwaters. In accordance with these beach changes, sand deposition west of the inlet continued, resulting in the widening of the shoal in the longshore direction. As a result, a large-scale trough west of the inlet, which was seen in 1985, was buried by sand, and the size of the concave trough decreased.

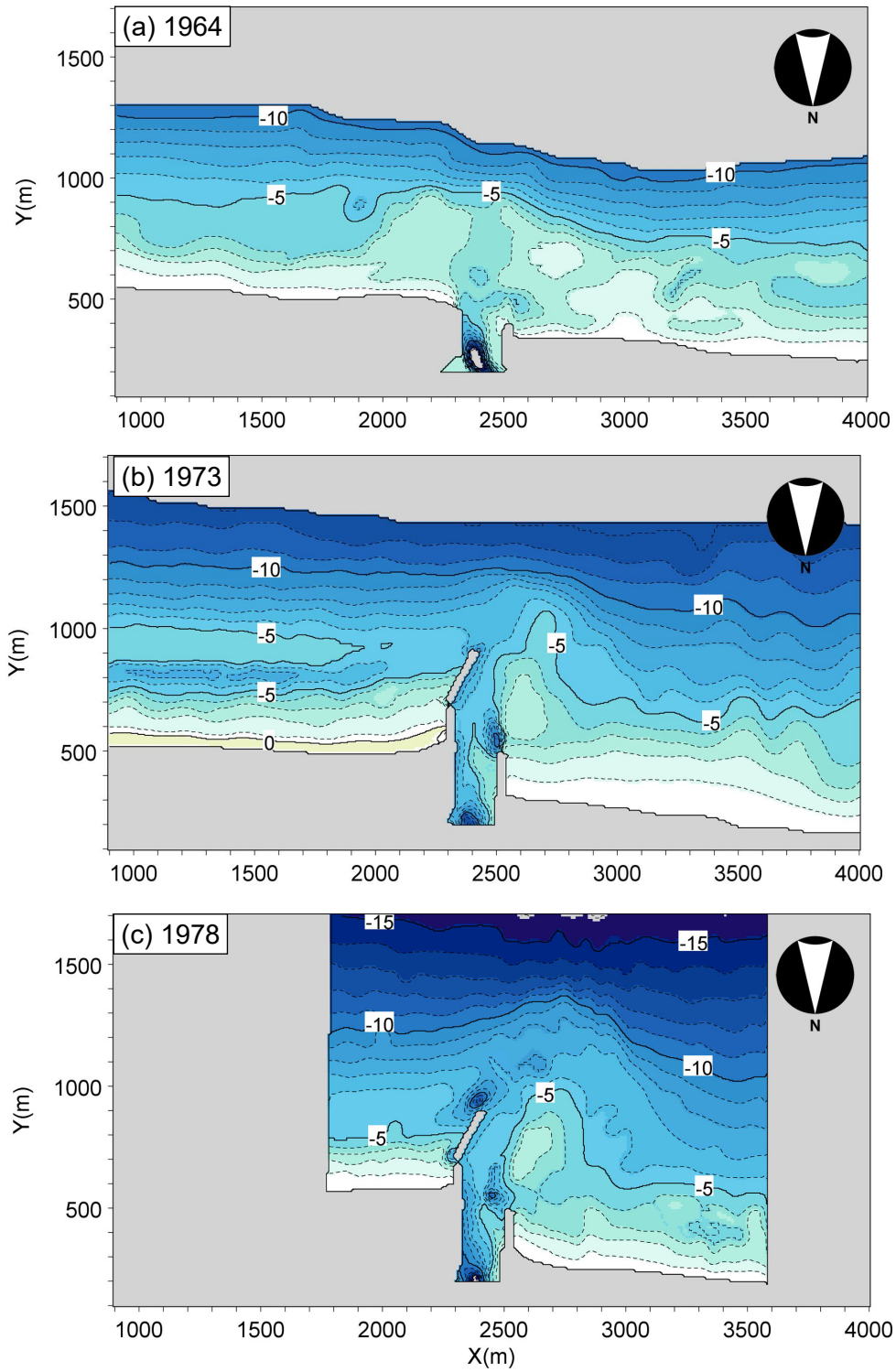


Figure 2. Bathymetries around Imagire-guchi inlet between 1964 and 2017.

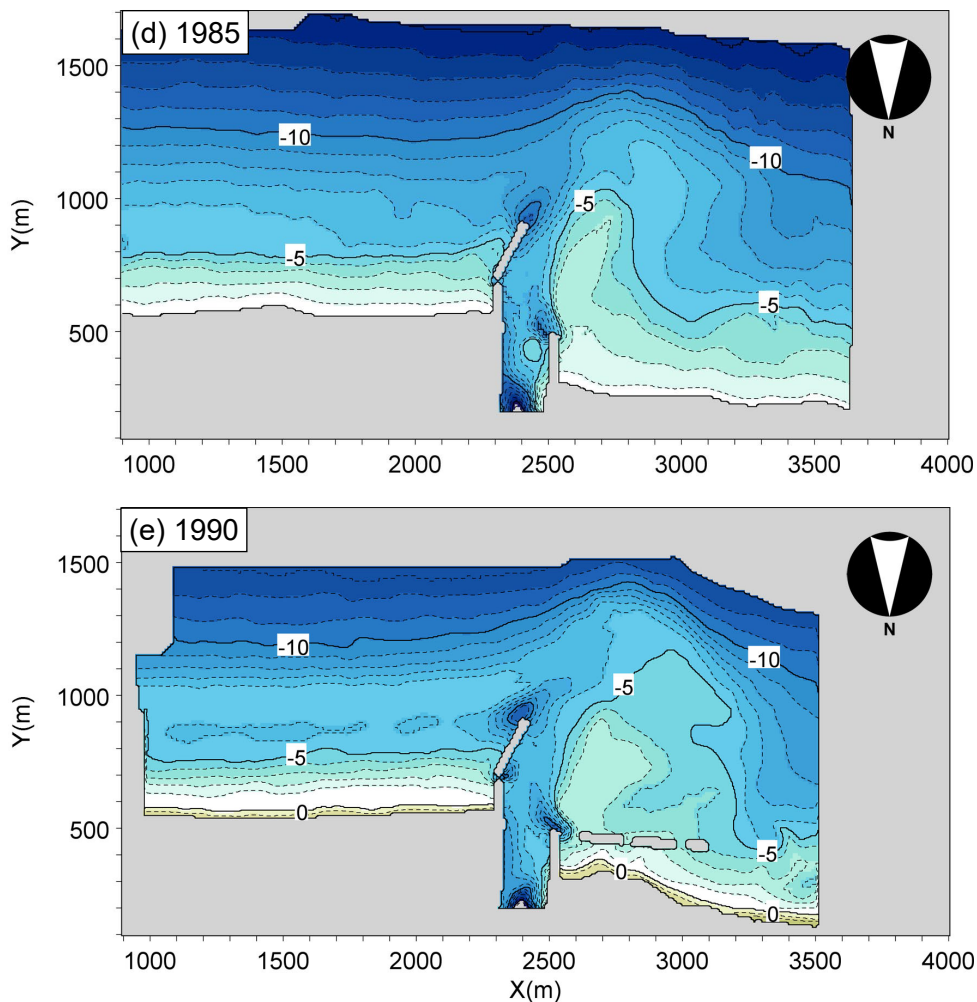


Figure 2. Bathymetries around Imagire-guchi inlet between 1964 and 2017 (continued).

By 1994, detached breakwater No. 3 of 150 m length at the west end had been completed, as shown in Fig. 2f, and the shoal, which had been developing immediately west of the inlet since 1985, further developed, and the trough that had extended since 1985 close to the shoreline disappeared. The offshore development of the ebb tidal delta further continued with the deposition of sand up to 14 m depth.

By 1998, a triangular shoal surrounded by the 5 m depth contour had formed immediately west of the inlet, by which the channel of the inlet was forced to move eastward along with the formation of an opening facing southeast, as shown in Fig. 2g. Because the tip of the training jetty was bent inward, the ebb tidal current concentrated at the tip, causing a deep scouring hole. By 2004, a triangular shoal had developed offshore of the three detached breakwaters, as typically designated by the 4 m depth contour, as shown on Fig. 2h, and an oblique trough was formed across the shoal west of the inlet where a flat seabed extended in the past. In addition, the depth at the tip of the foreset slope of the ebb tidal delta reached 14 m.

Then, by 2009, the 5 m depth contour retreated offshore of the detached breakwaters, and the shape of the contour became mild in the longshore direction, as shown in Fig. 2i. Because the point depth of the foreset slope of the ebb tidal delta reached 14 m, a large part of the westward longshore sand transport was trapped by the ebb tidal delta. In 2014, a triangular shoal bounded by the 5 m depth contour was formed offshore of the detached breakwaters, as shown in Fig. 2j, and a deep, oblique channel was formed along the east side of this triangular shoal with 5 m depth. Finally, by 2017, as shown in Fig. 2k, the 5-m-depth contour markedly protruded offshore of the detached breakwaters. Note that the size of the slender protruding sandbar immediately west of the inlet had markedly increased, although the shape of the ebb tidal delta was similar to that in 1985, as shown in Fig. 2d. By

2017, a large ebb tidal delta protruding offshore had formed with the tip of the foreset slope reaching 14 m depth.

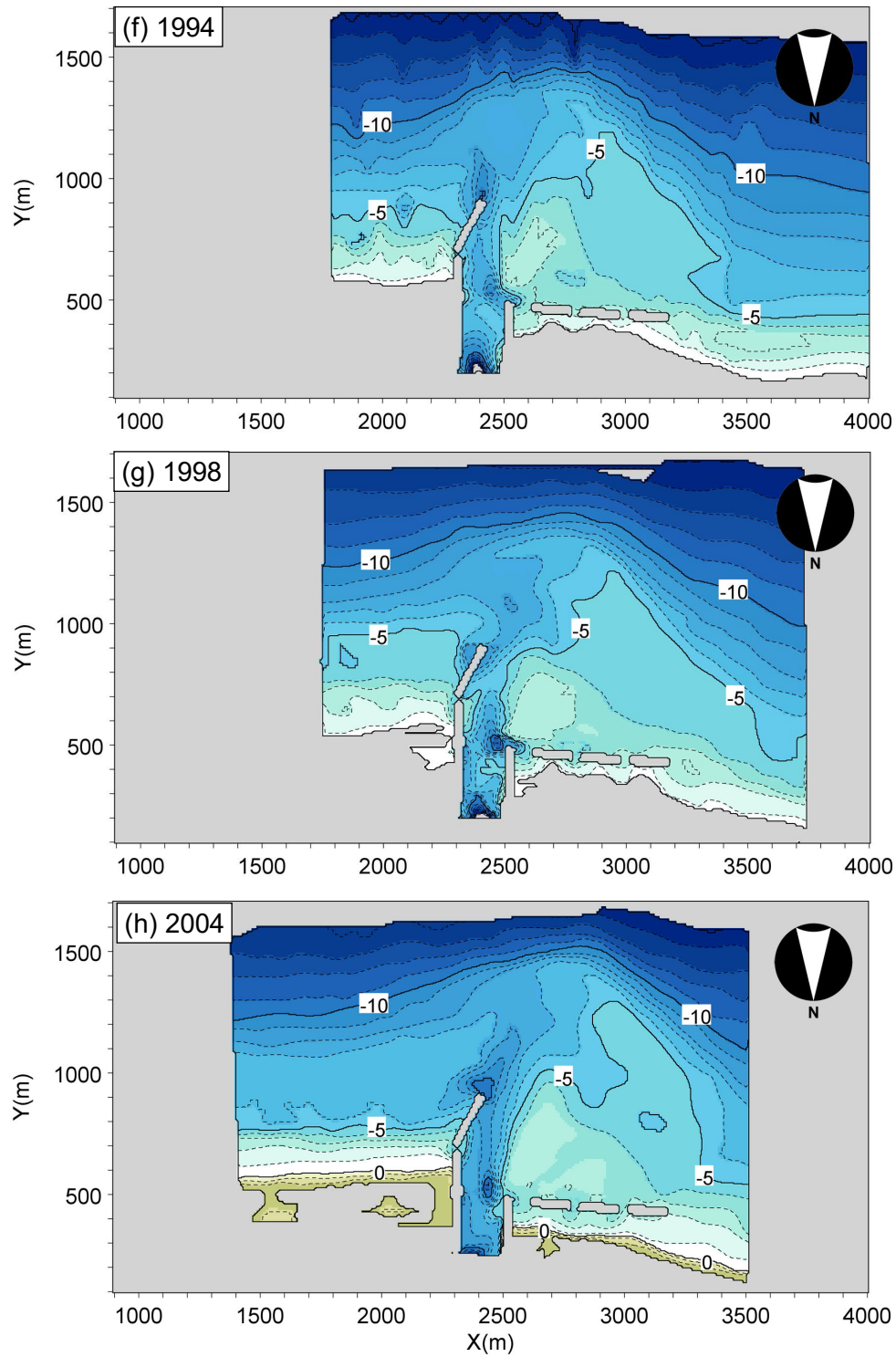


Figure 2. Bathymetries around Imagire-guchi inlet between 1964 and 2017 (continued).

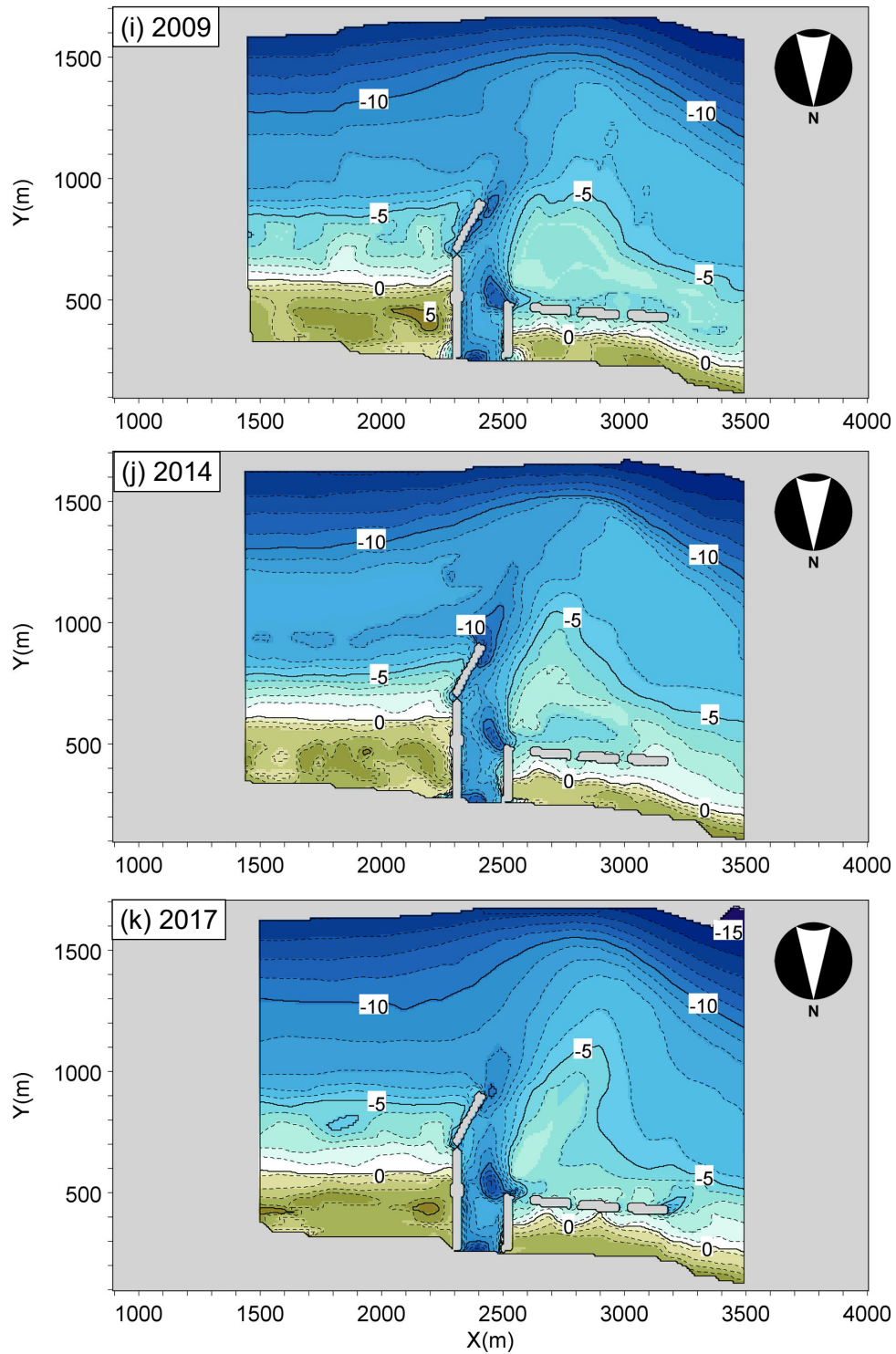


Figure 2. Bathymetries around Imagire-guchi inlet between 1964 and 2017 (continued).

BATHYMETRIC CHANGES RELATIVE TO BATHYMETRY IN 1978

Because bathymetric surveys were carried out in the same range around Imagire-guchi inlet since 1978, and dominant bathymetric changes were observed after 1978 when an oblique training jetty was extended, bathymetric changes were calculated eight times in the period between 1978 and 2017 with reference to the bathymetry in 1978. Figure 3 shows the bathymetry in selected years and the bathymetric changes.

In 1985, the primary deposition area was located in the area where the ebb tidal current that concentrated along the oblique jetty attenuates in the offshore zone, forming a sand deposition zone of elliptic shape in the depth zone between -6 and -14 m (Fig. 3a), whereas erosion occurred inside the inlet and in the zone shallower than -10 m east of the inlet. Furthermore, an erosion zone was formed in the depth zone between -4 and -9 m landward of the offshore deposition zone west of the inlet. By 1990, a sand deposition zone had markedly expanded offshore of the inlet (Fig. 3b), whereas severe beach erosion occurred immediately west of the detached breakwaters. Part of the westward longshore sand transport was transported obliquely in the offshore zone owing to the ebb tidal current, and sand was deposited offshore of the inlet. Not only did sand supply downcoast decrease by the amount that was transported offshore but also the protruding topography of the ebb tidal delta blocked the westward longshore sand transport. This explains the formation of the erosion zone immediately downcoast of the sand deposition zone.

In 1994, the sand deposition zone expanded to the area east of the training jetty in the offshore zone (Fig. 3c). Furthermore, this sand deposition zone expanded close to the detached breakwater west of the inlet, and a slender erosion zone was formed between this sand deposition zone and the detached breakwater. By 1998, the sand deposition zone had expanded further west of the detached breakwaters while enclosing the whole ebb tidal delta (Fig. 3d). At this stage, too, a small erosion zone was left in front of the sand deposition zone west of the detached breakwaters, implying that the formation of the erosion zone responded to the westward expansion of the sand deposition zone. It is concluded from the topographic changes between 1978 and 1998 that a sand deposition zone was formed offshore of the inlet, and it gradually expanded westward together with the formation of an erosion zone at its west end.

In 2004, a large amount of sand was deposited offshore of the inlet with a maximum thickness of 6.5 m (Fig. 3e). A slender sand deposition zone was formed along the 10 m depth contour, and a deep channel was formed inside the inlet. Furthermore, an erosion zone along the shoreline started to be formed on the east side of the training jetty beyond its tip. By 2009, the size of the sand deposition zone offshore of the inlet had increased (Fig. 3f), and simultaneously, a deep channel developed inside the inlet as well as a trough connecting the deep channel east of the training jetty. On the other hand, sand was accumulated behind the detached breakwaters, and the offshore deposition zone along the 10 -m-depth contour further extended. In 2014, the tip of the channel inside the inlet and the trough extending alongshore offshore of 5 m depth were buried with sand, resulting in a decrease in water depth (Fig. 3g). Finally, in 2017, a dominant sand deposition zone was formed in the offshore depth zone between -7 and -10 m with the development of the ebb tidal delta, whereas the seabed was markedly eroded inside the inlet and east of the training jetty (Fig. 3h).

As the occurrence mechanism of the topographic changes in the field, which is subject to strong ebb tidal current from the inlet, the flow pattern associated with the ebb tidal current around the inlet can be schematically drawn, as shown in Fig. 4. The strong ebb tidal current is forced to flow out in a straight line by the training jetty. The sand deposition zone offshore of the inlet was assumed to be formed by this oblique current. On the western side of the strong offshore current, shoreward current is induced, resulting in the formation of a large-scale circulation west of the inlet. The formation of a local scouring hole at the tip of the right-hand-side jetty is evidence of the formation of the circulating current. In the area along the west bank, a strong ebb tidal current and induced current flow out, so a deep channel was considered to be formed. Similarly, on the east side, a forced current is generated near the tip of the training jetty, and this flows directly offshore; the current field can be accelerated in the vicinity of the training jetty on the eastern side of the inlet by the ebb tidal current. Finally, topographic changes, as shown in Fig. 3h, were considered to be formed.

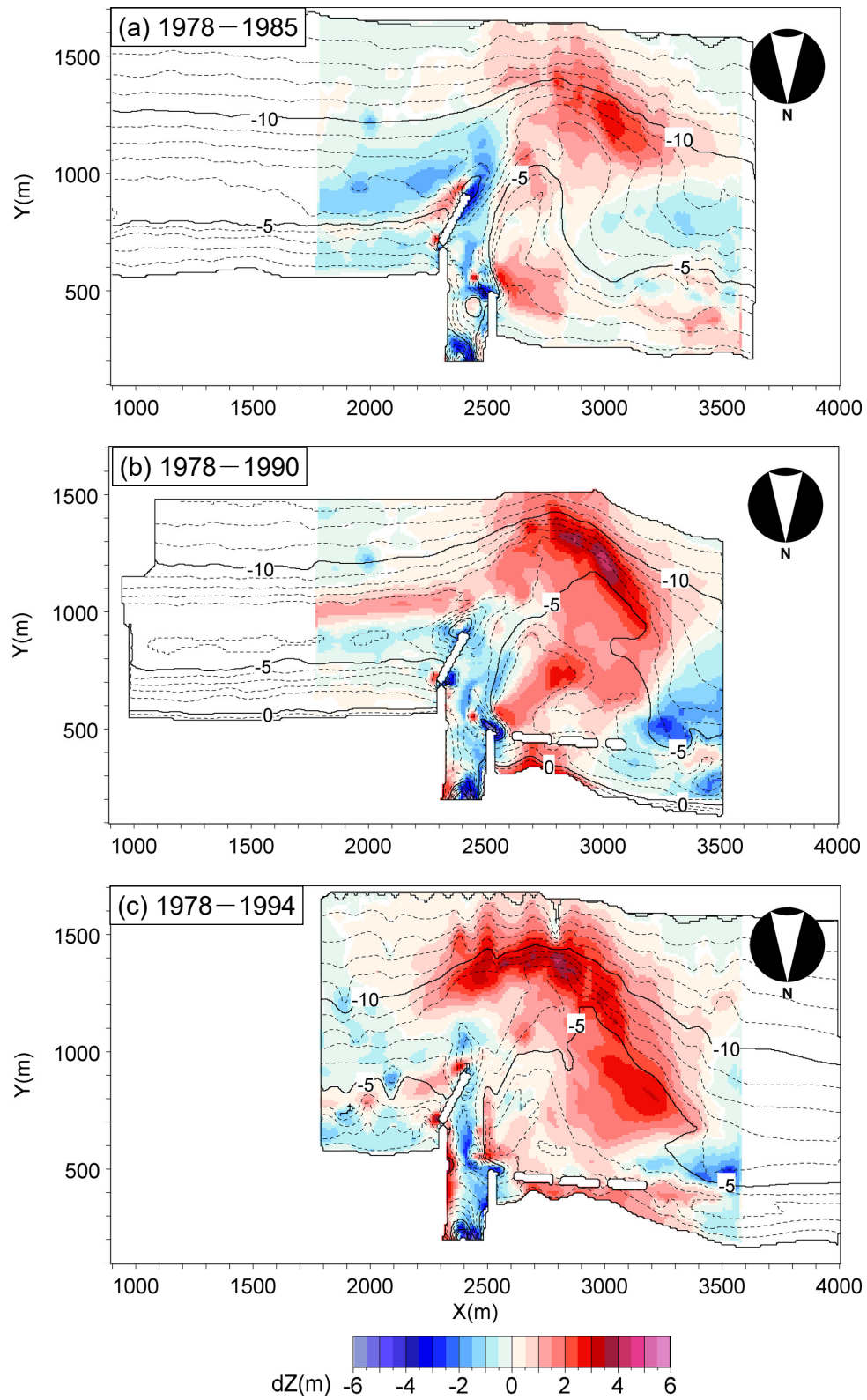


Figure 3. Bathymetric changes around Imagire-guchi inlet with reference to the bathymetry in 1978.

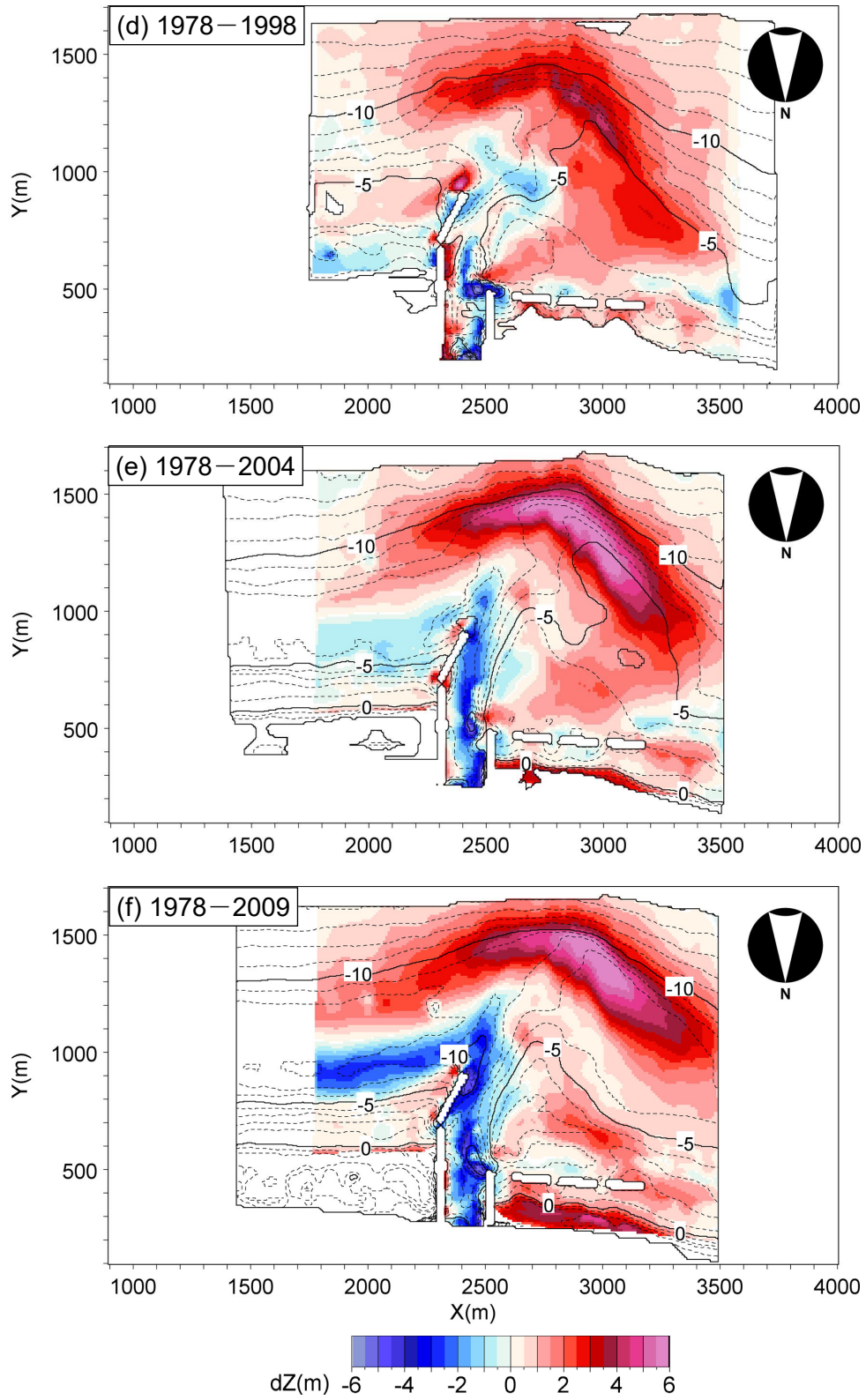


Figure 3. Bathymetric changes around Imagire-guchi inlet with reference to the bathymetry in 1978

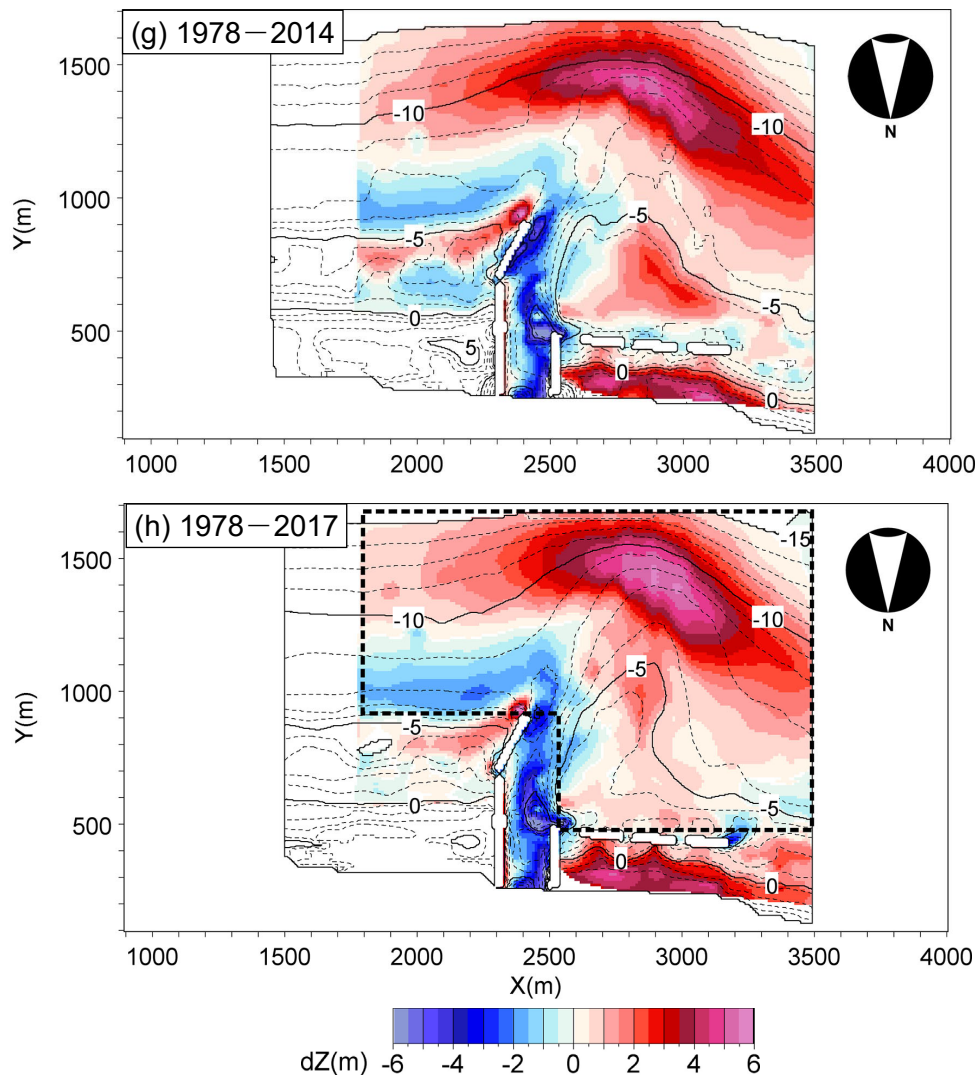


Figure 3. Bathymetric changes around Imagire-guchi inlet with reference to the bathymetry in 1978 (continued).

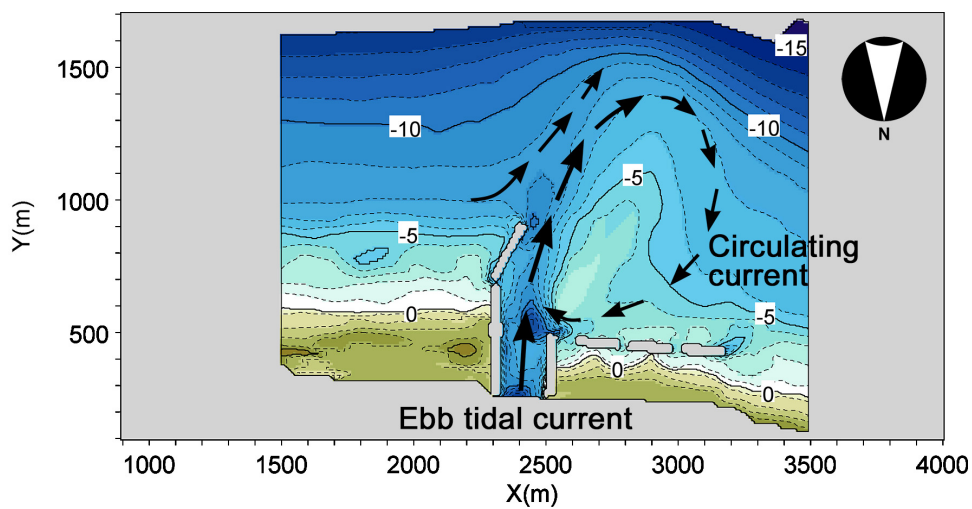


Figure 4. Schematic diagram of current in a field with strong ebb tidal current.

COMPARISON OF BATHYMETRIC CHANGES IN SELECTED PERIODS

In the previous section, topographic changes in eight years selected between 1978 and 2017 were investigated with reference to the initial topography in 1978. This method has an advantage in enabling investigation of the cumulative change in the seabed topography, but not the topographic changes in successive years. Therefore, topographic changes in the three periods of 1978–1990, 1990–2004, and 2004–2017 were investigated again. First, in the first period between 1978 and 1990, a primary sand deposition area was formed along the southwest side of the ebb tidal delta owing to the effect of an oblique training jetty, and the main deposition area was approximated by an oval, as shown in Fig. 5a. In the second period between 1990 and 2004, the sand deposition zone expanded in the east-west direction enclosing the entire inlet, and the west end of the detached breakwaters was included in the sand deposition zone, as shown in Fig. 5b. However, in the third period between 2004 and 2017, the sand deposition zone between 7 and 10 m depths, which was clearly seen between 1990 and 2004, disappeared, as shown in Fig. 5c. Instead, not only the thickness of the sand in the offshore sand deposition erosion zone decreased, but also the size of the trough landward of the sand deposition area markedly increased, and the offshore deposition zone expanded westward and moved offshore, resulting in the formation of the opening on the western side of the ebb tidal delta.

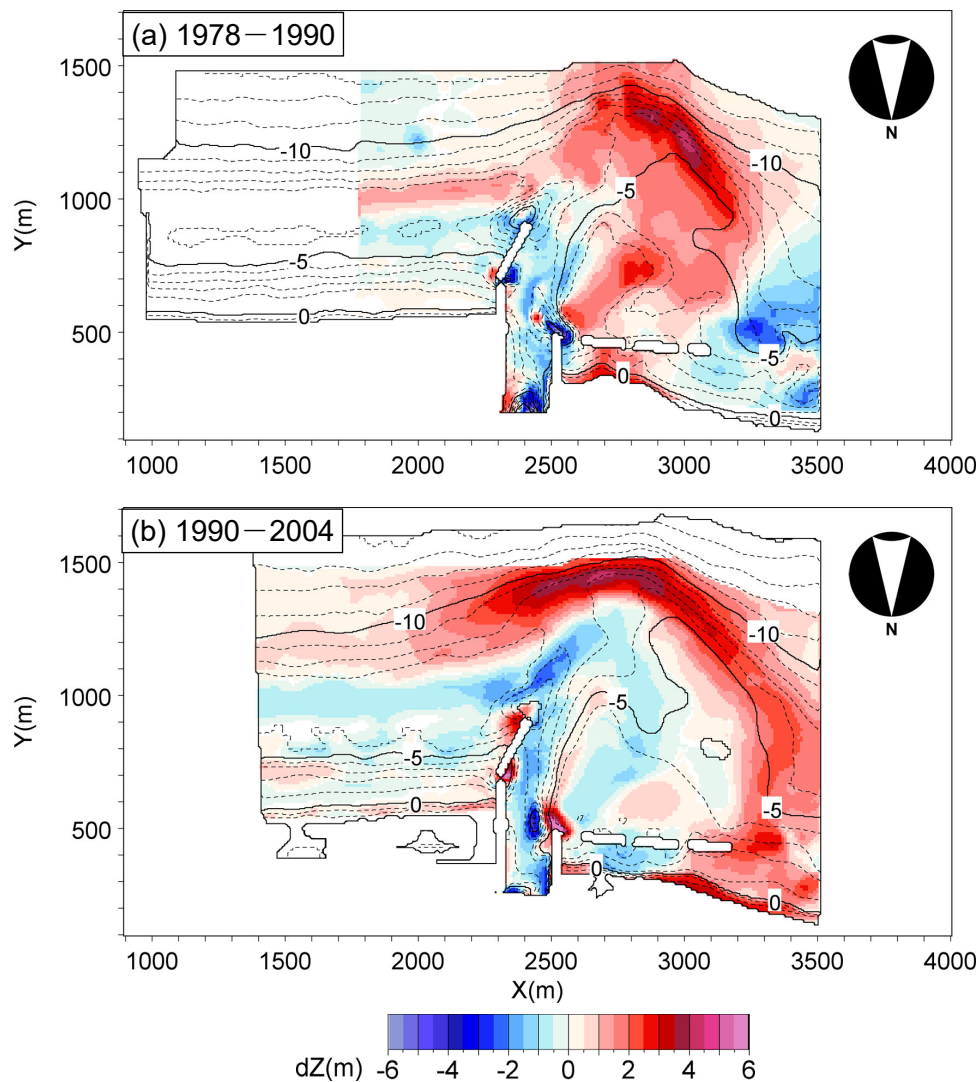


Figure 5. Planar distribution of bathymetric changes around Imagire-guchi inlet in selected years.

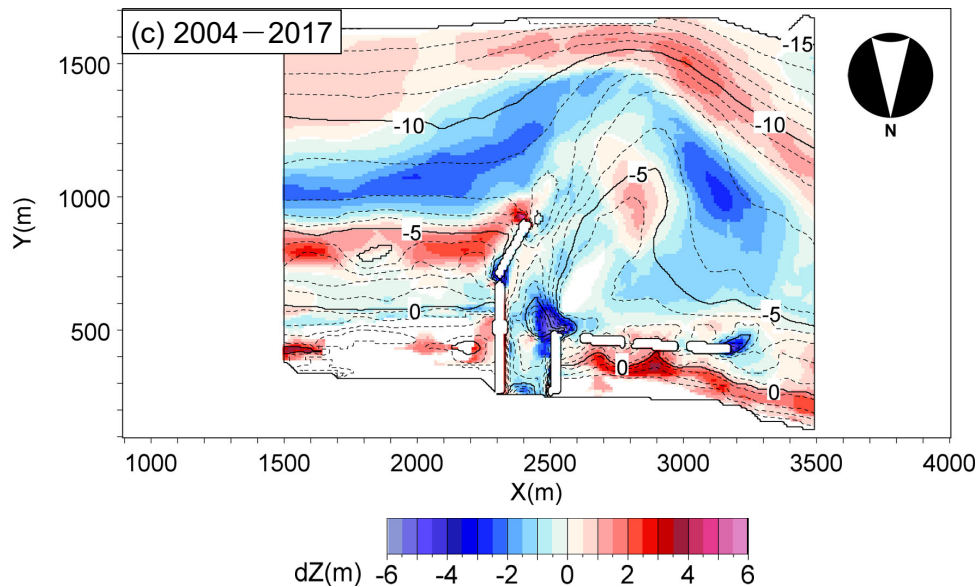


Figure 5. Planar distribution of bathymetric changes around Imagire-guchi inlet in selected years (continued).

CHANGES IN SAND VOLUME IN ENTIRE EBB TIDAL DELTA

By setting a calculation domain covering the entire ebb tidal delta offshore of the inlet, as shown in Fig. 3h, the changes in sand volume in consecutive years were calculated using the bathymetric survey data collected each year. In the calculation, the changes in sand volume in the entire study area and in the zones deeper and shallower than 10 m were separately calculated. Figure 6 shows the volume changes between 1962 and 2017 in the entire study area and in the zones deeper and shallower than 10 m. The dotted lines in the figure correspond to the long-term trend since 1964 determined by a linear regression analysis. The total volume of sand increased at a rate of $8.4 \times 10^4 \text{ m}^3/\text{yr}$ between 1964 and 2005, and then it began to decrease after 2005 at a rate of $4.3 \times 10^4 \text{ m}^3/\text{yr}$. The sand volume in the zone deeper than 10 m also monotonically increased at a rate of $3.4 \times 10^4 \text{ m}^3/\text{yr}$ since 1964 up to 2017 with no decrease. The sand volume in the zone shallower than 10 m also increased at a rate of $3.4 \times 10^4 \text{ m}^3/\text{yr}$ between 1964 and 2005, but it rapidly decreased at a rate of $7.3 \times 10^4 \text{ m}^3/\text{yr}$ after 2005. Thus, the decrease in sand volume of the entire study area after 2005 was mainly attributable to the decrease in the zone shallower than 10 m, because the sand volume in the zone deeper than 10 m continuously increased at a rate of $3.4 \times 10^4 \text{ m}^3/\text{yr}$. Taking into consideration of the fact that the zone with the depth shallower than 10 m is where longshore sand transport prevails, the decrease in sand volume in the zone shallower than 10 m is considered to be caused by the spatial imbalance in westward longshore sand transport. The decrease in sand volume in the study area between 2004 and 2017 is considered to be mainly due to the erosion in the zone shallower than 10 m, as shown in Fig. 6.

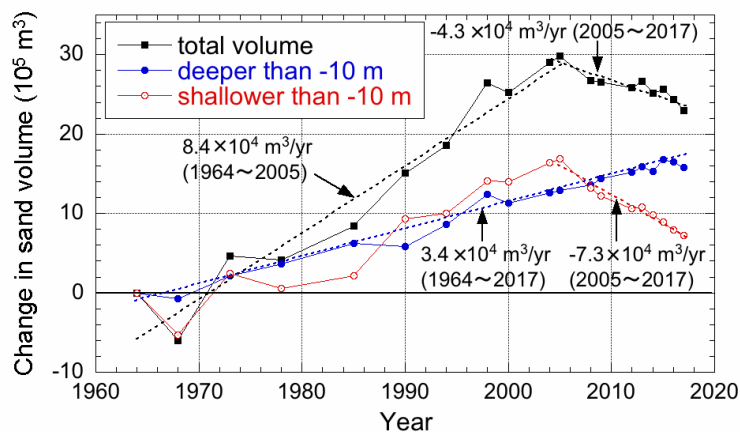


Figure 6. Change in sand volume in study areas with reference to the bathymetry in 1964.

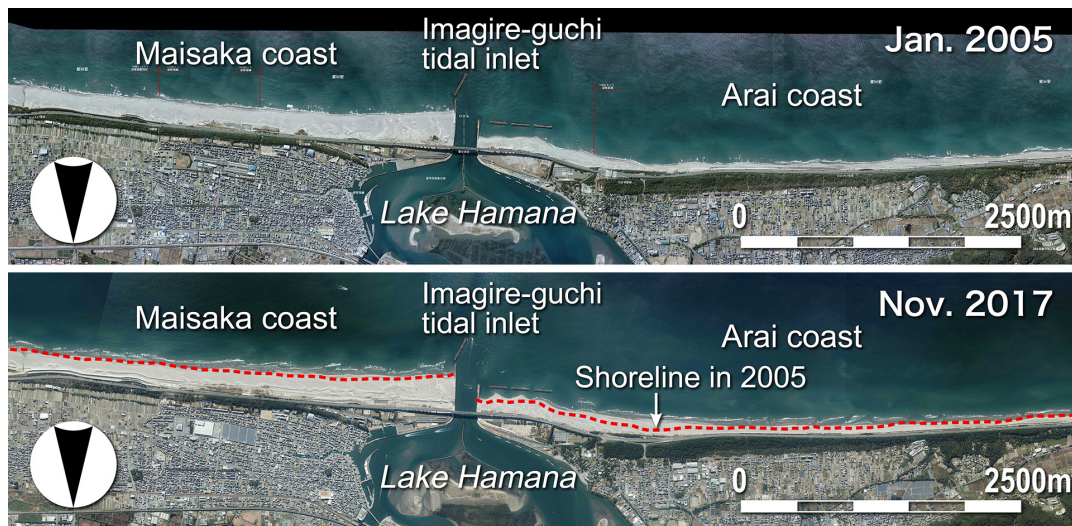


Figure 7. Shoreline changes until 2017 relative to that in 2005.

CONCLUSIONS

The bathymetric responses of Imagire-guchi tidal inlet to the extension of an oblique training jetty were investigated using the bathymetric survey data collected 11 times between 1964 and 2017. It was found that the total volume of sand in the ebb tidal delta decreased at a rate of $4.3 \times 10^4 \text{ m}^3/\text{yr}$ after 2005, although the total volume of sand deposited offshore of this inlet increased at a rate of $8.4 \times 10^4 \text{ m}^3/\text{yr}$ between 1964 and 2005 owing to the ebb tidal current. Furthermore, sand was depositing at a rate of $3.4 \times 10^4 \text{ m}^3/\text{yr}$ in the zone deeper than 10 m after 2005, whereas the seabed was eroded at a rate of $7.3 \times 10^4 \text{ m}^3/\text{yr}$ in the zone shallower than 10 m. This difference in the rates is considered to be due to the sand discharge by westward longshore sand transport. Assuming that the entire westward sand transport through the inlet temporarily decreased to 0 during the period when the ebb tidal delta had rapidly developed until 2005, similarly to that described by Kainuma et al. (2018), the rate of sand supply by westward longshore sand transport to the inlet became $8.4 \times 10^4 \text{ m}^3/\text{yr}$, as shown in Fig. 6. The sand supply downcoast (the Arai coast) after 2005 can be calculated by subtracting the sand loss at a rate of $3.4 \times 10^4 \text{ m}^3/\text{yr}$ toward the zone deeper than 10 m, and by adding the rate of sand supply of $7.3 \times 10^4 \text{ m}^3/\text{yr}$ from the erosion in the zone shallower than 10 m. Thus, the sand supply downcoast became $12.3 \times 10^4 \text{ m}^3/\text{yr}$ in total. This value is in good agreement with the longshore sand transport of $12.1 \times 10^4 \text{ m}^3/\text{yr}$ estimated at a location 6 km west of the inlet (Kainuma et al., 2018). The increase in sand supply by longshore sand transport to the Arai coast after 2005 corresponds to the shoreline advance up to 50 m between 2005 and 2017, as shown in Fig. 7.

It is concluded that a large-scale ebb tidal delta developed offshore of Imagire-guchi tidal inlet after the extension of a training jetty owing to the ebb tidal current, and at present, sand is still depositing at a rate of $3.4 \times 10^4 \text{ m}^3/\text{yr}$ to the foreset slope of the ebb tidal delta, which constitutes the net loss of sand in the nearshore zone in terms of shore protection. Although the development of the ebb tidal delta still continues, sand discharge by westward longshore sand transport has been occurring in the zone shallower than 10 m since 2005, and the sand is supplied downcoast. Approximately the same amount of longshore sand transport as that before the construction of Imagire-guchi tidal inlet was found, implying that the bathymetry around the inlet is approaching a dynamically stable beach.

REFERENCES

- Kainuma, M., Hakamata, M., Nagai, T., Uda, T., and Ishikawa, T. 2018. Shoreline changes on Hamatsu-goto and Kosei coasts facing Enshu-nada Sea and evaluation of longshore sand transport, Proc. JSCE B3 (Civil Eng. in the Ocean), Vol. 74, No. 2, pp. I_671-I_676. (in Japanese)
- Tung, T. T., Stive, M. J. F., van de Graaff, J. and Walstra, D. J. R. 2007. Morphological behavior of seasonal closure of tidal inlets, Coastal Sediments '07, pp. 1589-1600.
- Uda, T., Serizawa, M., and Miyahara, S. 2018. Morphodynamic model for predicting beach changes based on Bagnold's concept and its applications, INTEC, London, UK.
<https://www.intechopen.com/books/morphodynamic-model-for-predicting-beach-changes-based-on-bagnold-s-concept-and-its-applications>